



Characterization of Correction Factors to Enable Assessment of Clinical Risk from In Vitro CYP3A4 Induction Data and Basic Drug-Drug Interaction Models

Diane Ramsden^{1,3} · Cody L. Fullenwider²

Accepted: 23 February 2022 / Published online: 28 March 2022
© The Author(s) 2022

Abstract

Background and Objective Induction of drug-metabolizing enzymes can lead to drug-drug interactions (DDIs); therefore, early assessment is often conducted. Previous reports focused on true positive cytochrome P450 3A (CYP3A) inducers leaving a gap in translation for in vitro inducers which do not manifest in clinical induction. The goal herein was to expand the in vitro induction dataset by including true negative clinical inducers to identify a correction factor to basic DDI models, which reduces false positives without impacting false negatives.

Methods True negative clinical inducers were identified through a literature search, in vitro induction parameters were generated in three human hepatocyte donors, and the performance of basic induction models proposed by regulatory agencies, concentration producing twofold induction (F_2), basic static model (R_3) and relative induction score (RIS), was used to characterize clinical induction risk.

Results The data demonstrated the importance of correcting for in vitro binding and metabolism to derive induction parameters. The aggregate analysis indicates that the RIS with a positive cut-off of < 0.7 -fold area under the curve ratio (AUCR) provides the best quantitative prediction. Additionally, correction factors of ten and two times the unbound peak plasma concentration at steady state ($C_{\max,ss,u}$) can be confidently used to identify true positive inducers when referenced against the concentration resulting in twofold increase in messenger ribonucleic acid (mRNA) or using the R_3 equation, respectively.

Conclusions These iterative improvements, which reduce the number of false positives, could aid regulatory recommendations and limit unnecessary clinical explorations into CYP3A induction.

Diane Ramsden and Cody L. Fullenwider contributed equally to this work.

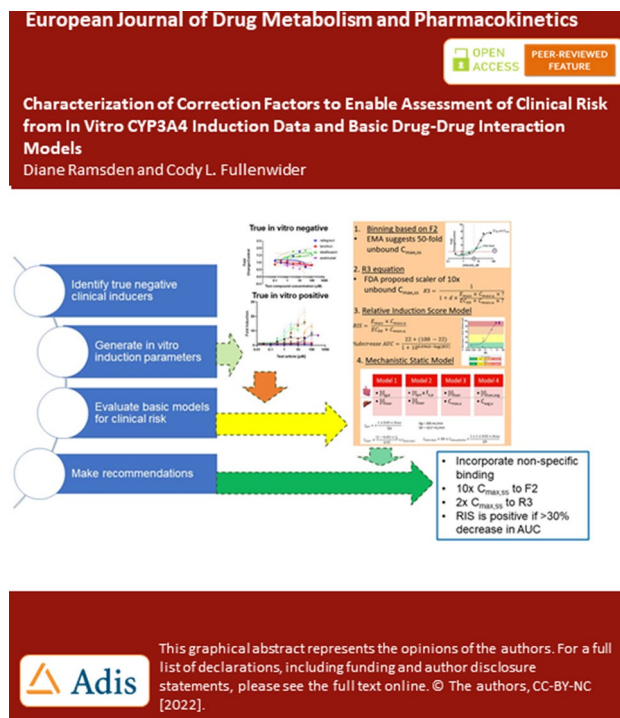
✉ Diane Ramsden
diane.ramsden@astrazeneca.com

¹ Takeda Development Center Americas, Inc., Cambridge, MA, USA

² Takeda Development Center Americas, Inc., San Diego, CA, USA

³ Present Address: Department of Oncology Research and Early Development, Drug Metabolism and Pharmacokinetics, AstraZeneca, 35 Gatehouse Park, Waltham, MA 02451, USA

Graphical abstract



Key Points

Collectively, the data demonstrate that in vitro-derived induction parameters from CYP3A4 mRNA level changes can be confidently used with basic models to evaluate clinical induction potential. Further correction factors are proposed, which, when applied to basic equations, can reduce the number of false positives, more accurately predict true positives and negatives for binning and improve the quantitative translation of induction based DDI risk

1 Introduction

There is a need to assess the DDI potential of compounds by evaluating their propensity to inhibit or induce cytochrome P450 (CYP) enzymes, Phase II enzymes and transporters. If a compound is a CYP inducer, the resulting increase of enzyme can lead to increased biotransformation of itself (autoinduction) or co-medicants. The primary mechanism by which drugs cause enzyme induction is by the activation of gene transcription. Therefore, to assess induction of metabolizing enzymes and transporters through receptor-mediated

agonism of PXR (i.e., CYP3A4, CYP2C9, P-gp, UGT), CAR (i.e., CYP2B6, CYP2Cs, SULT, UGT) and AhR (i.e., CYP1A2, UGT1A1, SULT1A1), cryopreserved human hepatocytes are often used, with known positive inducers, to provide confidence in the performance of the in vitro model. It is well accepted that the mechanisms underlying induction are consistent with other pharmacological processes, and, as such, characterizing the concentration response is an integral part of risk assessment. Regulatory agencies recommend that the induction potential of a new chemical entity (NCE) be evaluated using plated human hepatocytes from three separate donors. They further propose basic equations to be used to evaluate the clinical risk based on the in vitro-derived induction parameters (Table S1). The equations are referred to as $F2$, $R3$ and relative induction score (RIS) and employ the induction parameters, including the concentration resulting in twofold increase in mRNA ($F2$), the concentration resulting in half maximal fold induction (EC_{50}) and the maximal fold induction (E_{max}), derived from nonlinear fitting of mRNA fold changes referenced to a housekeeping gene. Due to the importance of CYP3A in the metabolism of xenobiotics as well as the clinical precedence of strong induction, many recommendations have focused on CYP3A [1–4]. Although work on the translation of in vitro data for other enzymes has been conducted, it remains limited [5, 6]. Recently, a large dataset for clinically relevant CYP3A inducers was collected and analyzed as part

of the International Consortium for Quality, Induction Working Group (IQ-IWG)'s efforts; however, there were minimal data for in vitro inducers that are not also in vitro inhibitors and clinical induction is negative. Therefore, the goal of this work was to expand the true negative dataset, using clinical data for selective CYP3A substrates, to develop recommendations to basic models (*F2*, *R3* and *RIS*) for interpreting their induction risk.

2 Materials and Methods

2.1 Chemicals and Reagents

Williams E Media, Hepatocyte Thawing Medium (HTM), Hepatocyte Thaw and Plate Supplement (HTPM), Primary Hepatocyte Maintenance Medium Supplement (PHMM), Hanks' Balanced Salt Solution (HBSS), Geltrex™ LDEV-Free hESC-Qualified, Reduced Growth Factor Basement Membrane Matrix, Collagen-I-coated 96-well plates, mRNA Catcher™ PLUS Purification Kit, TaqMan™ Reverse Transcription Reagents, TaqMan™ Fast Advanced Master Mix and TaqMan™ Gene Expression Assay (hGAPDH HS99999905_m1, CYP3A4 HS00604506_m1) were obtained from Life Technologies, (Carlsbad, CA, USA). Chemicals acebilustat, delafloxacin, lesinurad, raltegravir rifaximin rilpivirine, tafamidis, tasimelteon and tenofovir were acquired from Millipore Sigma (St. Louis, MO, USA). Binimetinib, doravirine, selexipag/NS 304 and sofosbuvir were from Thermo Fisher Scientific, (Waltham, MA, USA). Human cryopreserved hepatocytes were obtained from Bioreclamation In Vitro Technologies (Baltimore, MD, USA). All other reagents were of sufficient grade or purity.

2.2 Identification of True Negative Clinical Inducers

To identify true negative clinical inducers, for derivation of in vitro induction kinetic parameters, a targeted search using the University of Washington Drug-Drug Interaction database (UW-DIDB) was conducted. All clinical studies testing an effect (inhibition, no inhibition, induction, no induction or other PK interactions) were collected for the sensitive substrates highlighted in Table S2. Both positive (area under the curve ratio [AUCR] < 0.8) and negative (AUCR ≥ 0.8) clinical induction studies were collated for comparisons. Additionally, positive and negative clinical inhibition studies for the same substrate set were included to cross check whether the negative inducers resulted in any relevant clinical inhibition. Once the test set was identified, the literature and UW-DIDB were searched for in vitro induction and inhibition parameters.

2.3 Culture of Cryopreserved Human Hepatocytes

Human cryopreserved hepatocytes from both male and female donors of differing age and racial origin are illustrated in Table S3 and treated as previously described with minor modifications [7]. In short, cryopreserved hepatocytes were thawed for 1.5 to 2 min using a 37 °C water bath and combined with HTM prewarmed to 37 °C. The tube was capped and gently inverted four times to mix cells followed by centrifugation at 100g for 10 min. Following centrifugation, supernatant was carefully aspirated without disturbing the pellet. Cells were re-suspended by the addition of 2–3 ml per vial in HTPM. Cells were manually counted by trypan blue exclusion and resuspended to a final viable cell count of 1.2×10^6 cells/ml in HTPM. Prior to plating, Collagen-I coated 96-well plates wells were pre-wet with 50 µl HTPM and prewarmed to 37 °C. To seed plates, 50 µl cell suspension was added to the prewet warmed plates to achieve a final seeding density of 6.0×10^4 cells/well. Cells were distributed within the well by sliding the plate approximately 2 inches in a north, south, east, west (↑↓→←) direction from center and placed in a humidified incubator at 37 °C with 5% CO₂. Following an approximate 4-h attachment period, plates were removed and media was aspirated to remove any non-attached hepatocytes and cellular debris. Sandwich cultures were constructed by the addition of 100 µl ice cold PHMM containing 0.35 mg/ml Geltrex. Plates were returned to a 37 °C, 5% CO₂ humidified incubator for ~ 20 h. Compounds were dissolved in DMSO and added to the PHMM at various concentrations, Table S4 (final DMSO concentration, 0.1%), and incubations were conducted in triplicate. Treatment with test compound, vehicle or prototypical inducers was initiated ~ 24 h after seeding. Media were aspirated and replaced with fresh media containing test article at 48 h post-seeding. On the 2nd day of treatment, metabolic stability was characterized by the removal of aliquots from the remaining dosing solutions to serve as “0 min,” and media samples were collected at 4 and 24 h. Cell viability was assessed by visual inspection of the monolayer, checking for confluency and morphology. After a total treatment time of 48 h, the medium was removed, and the cells were washed with 100 µl HBSS. After washing, HBSS was aspirated and plates were sealed and stored at – 80 °C prior to RNA isolation.

2.4 Determination of Relative mRNA Levels

The cells were lysed using lysis buffer and prepared for RNA isolation. After the isolation of RNA using commercially available kits, cDNA was synthesized using standard polymerase chain reaction (PCR) protocols. CYP3A4

and an endogenous housekeeping gene glyceraldehyde-3-phosphate dehydrogenase (GAPDH) were quantified by real-time PCR. The gene-specific primer/probe sets were obtained from Applied Biosystems, and real-time PCR was performed using CYP3A4 and the endogenous control target cDNAs. The relative quantity of the target cDNA compared with that of the endogenous control was determined by the $\Delta\Delta$ threshold cycle method (Applied Biosystems User Bulletin 2). Threshold cycle values > 32 were excluded from the analysis. Relative quantification measured the change in mRNA expression in test samples relative to that in vehicle control sample (0.1% DMSO).

2.5 LC-MS/MS Analysis

The system used for LC-MS/MS analysis consisted of an ExionLC HPLC system and a Triple Quad 4000 or 4500 tandem mass spectrometer (AB Sciex, Framingham, MA). A 10- μ l aliquot of sample was injected for analysis using the peak area ratio of analyte compared to proprietary internal standard (m/z 468.919 \rightarrow 133.089 IS POS or 467.22 \rightarrow 85.00 IS NEG). High-performance liquid chromatography separation was accomplished using Kinetex XB-C18 column (2.1 \times 50 mm, 5 μ m; Phenomenex, Torrance, CA). Mobile phase A consisted of 0.1% formic acid in water, and mobile phase B was 0.1% formic acid in acetonitrile. Analyte-specific gradient conditions and multiple reaction monitoring MS/MS details are presented in Supplemental Table S5.

2.6 Equations

The AUC_{0-24h} ($AUC_{all(Cobs)}$) was calculated using the linear trapezoidal rule (Eq. (1)), and the average concentration over the last day of dosing was calculated by dividing the AUC_{0-24h} by 24 h.

$$AUC_{all(Cobs)} = \sum_{i=0}^{n-1} \frac{(C_i + C_{i+1}) \times (t_{i+1} - t_i)}{2} \quad (1)$$

The free fraction of each test article in culture medium, $f_{u, \text{in vitro}}$, was estimated using Eq. (2), where $F_{unbound}$ and F_{bound} refer to the unbound fraction and bound fraction of drug in culture medium or plasma, and [ALBUMIN] refers to the albumin concentration in plasma (42.5 mg/ml) or in incubation medium (1.25 mg/ml). There are several assumptions made when applying this equation including that (1) the plasma protein binding is primarily to albumin, (2) there is one binding site on albumin and (3) the binding affinity is similar between bovine serum albumin and human serum albumin.

$$\text{Binding affinity} = \frac{[\text{ALBUMIN}] \times F_{unbound}}{F_{bound}} \quad (2)$$

2.7 Estimation of EC_{50} and E_{max} Parameters from In Vitro mRNA Hepatocyte Data

Concentration dependence was evaluated using standard linear regression and Spearman's nonparametric rank correlation coefficient. If the r value from Spearman's was positive with a significant p -value (< 0.05) and/or the slope

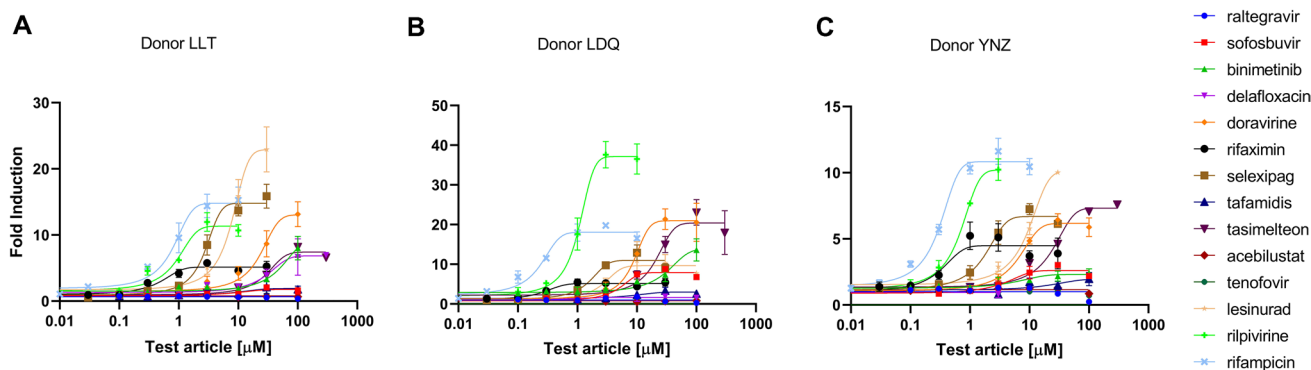


Fig. 1 Concentration response curves for clinically negative CYP3A4 inducers. The fold increase in CYP3A mRNA level (y-axis) was plotted against concentration (x-axis) to derive the in vitro induction parameters. Each datapoint represents the mean and standard deviation for $n = 3$. Raltegravir is represented by a blue circle, sofosbuvir by a red square, binimetinib by a green upward triangle, delafloxacin by a purple upside-down triangle, rifaximin by a black circle of a larger size, selexipag by a brown square of a larger size, tafamidis

by a blue upward triangle of a larger size, tasimelteon by a darker purple upside-down triangle of a larger size, acebilstat by a maroon diamond, tenofovir by a small hunter green circle, lesinurad by a small yellow star, rilpivirine by a small green cross and rifampicin

of the simple linear regression model was positive, and the 95% confidence intervals did not contain zero, then non-linear regression curve fitting was performed. This step was adopted from [8] and is based on a decision tree to evaluate time-dependent inhibitors [9].

Induction parameters were determined using nominal (recovered) concentrations or the average concentration over the last 24 h, with and without consideration of the estimated $f_{u,in\ vitro}$. F2 was calculated by solving Eq. (3) for the concen-

$$\frac{AUC_i}{AUC} = \frac{1}{F_g + (1 - F_g) \times \left(\sum_{k=1}^n \frac{fm(E)_{g,k}}{C_{g,k}} + 1 - \sum_{k=1}^n fm(E)_{g,k} \right)} \times \frac{1}{\sum_{k=1}^n \frac{fm(E)_{h,k}}{C_{h,k}} + (1 - \sum_{k=1}^n fm(E)_{h,k})} \quad (8)$$

tration that resulted in twofold increase in mRNA level. The clinical relevance of induction potential was assessed by calculating the R3 value using Eq. (4), described in the final US Food and Drug Administration (FDA) DDI guidance [10] and Pharmaceutical and Medical Devices Agency (PMDA) Drug Interaction Guideline [17]. In line with the European Medicines Agency (EMA) guideline, the $F2/C_{max,ssu}$ was calculated, and cut-off values were evaluated. In addition, previously determined RIS equations were used to evaluate generic RIS models (Eqs. 5 and 6).

$$Y = E_{max} / (1 + \exp(-(X - EC_{50})/b)) \quad (3)$$

Y is the relative fold induction, b , is the hill slope, $[X]$ is the test article concentration, EC_{50} is the concentration eliciting half-maximal induction, and E_{max} is the maximum fold induction. In Eq. (4), X is the correction factor applied to the $C_{max,u}$ and d is the scaling factor and assumed to be 1; $C_{max,u}$ is the maximal unbound plasma concentration of the inducer.

$$R3 = \frac{1}{1 + d \times \frac{E_{max} \times C_{max,u} \times X}{EC_{50} + C_{max,u} \times X}} \quad (4)$$

$$RIS = \frac{E_{max} \times C_{max,u}}{EC_{50} + C_{max,u}} \quad (5)$$

$$\% \text{ decrease AUC} = \frac{22 + (100 - 22)}{1 + 10^{0.0963 - \log(RIS)}} \quad (6)$$

The mechanistic static model previously reported [11, 12] was also used, Eq. (7).

$$\frac{AUC_i}{AUC} = \frac{1}{F_g + (1 - F_g) \times \left(\sum_{k=1}^n \frac{fm(E)_{g,k}}{A_{g,k} \times B_{g,k} \times C_{g,k}} + 1 - \sum_{k=1}^n fm(E)_{g,k} \right)} \times \frac{1}{\sum_{k=1}^n \frac{fm(E)_{h,k}}{A_{h,k} \times B_{h,k} \times C_{h,k}} + (1 - \sum_{k=1}^n fm(E)_{h,k})} \quad (7)$$

where A is the reversible inhibition, B is the time-dependent inhibition, C is the induction, g is the gut, h is the liver, and k is the enzyme.

Since the enclosed analysis specifically identified inducers which were not reported to be inhibitors, the inhibition portions (reversible and time dependent) of the equation were removed, resulting in Eq. (8), which includes Eqs. (9) and (10), representing the induction in gut and liver, respectively.

$$C_{g,k} = \frac{1}{1 + \frac{d \times E_{max} \times I_{gut}}{I_{gut} + EC_{50}}} \quad (9)$$

$$C_{h,k} = \frac{1}{1 + \frac{d \times E_{max} \times I_{liver}}{I_{liver} + EC_{50}}} \quad (10)$$

Calculation of I_{gut} and I_{liver} was conducted using Eqs. 11, 12 and 13, respectively.

$$I_{gut} = \frac{1 \times Ka \times Dose}{Qg} \quad (11)$$

$$I_{liver} = \frac{(1 - H) \times f_u}{Rb} \times I_{inlet,max} \quad (12)$$

$$I_{inlet,max} = Rb \times C_{max,plasma} + \frac{Fa \times Fg \times Ka \times Dose}{Qh} \quad (13)$$

where blood flow in the gut (Qg) = 300 ml/min, blood flow in the liver (Qh) = 1.62 l/min, H is the hematocrit and assumed to be 0.45 and R_b is the blood-to-plasma ratio. F_a is the fraction absorbed, F_g is the fraction escaping gut metabolism, and ka is the absorption rate constant assumed in the analysis to be 1, 1 and 0.03 min^{-1} , respectively.

Consistent with work recently published, evaluating time-dependent inhibition of CYP3A, multiple iterations of the above model with various $[I]$ input values were considered [13], Fig. S1.

Model 1: Using gut concentration and unbound hepatic inlet as input parameters as described in regulatory guidance.

Model 2: Inputting gut concentration corrected with $f_{u,p}$ and unbound hepatic inlet.

Model 3: Inputting unbound hepatic inlet as the gut concentration and unbound $C_{\max,ss}$ as the hepatic concentration.

Model 4: Inputting the unbound average hepatic inlet concentration as the gut concentration and the average unbound concentration as the hepatic concentration.

Models were evaluated with published F_m values (Supplemental Table S12).

Equations presented in [14] were used to describe the clinical study impact of in vitro risk assessment.

The accuracy of the individual models was evaluated by deriving the geometric mean fold error (GMFE) according to Eq. (14).

$$\text{GMFE} = 10^{\text{mean}\left(\left|\log\frac{\text{predicted DDI}}{\text{observed DDI}}\right|\right)} \quad (14)$$

The root mean square error (RMSE) was calculated according to Eq. (15).

$$\text{RMSE} = \sqrt{\frac{\sum(\text{predicted DDI} - \text{observed DDI})^2}{\text{number of predictions}}} \quad (15)$$

3 Results

3.1 Identification of Clinically Negative Inducers for Derivation of Induction Parameters

Seventeen candidates were identified for in vitro evaluation including raltegravir, lesinurad, lersivirine, perampanel, flumazenil, sofosbuvir, tenofovir, rilpivirine, binimetinib, brivaracetam, delafloxacin, doravirine, rifaximin, selexipag, tafamidis, tasimelteon and acebilustat. Data for lersivirine, perampanel and flumazenil were available from [4], and brivaracetam was not commercially available. Searching the literature and the UW-DIDB confirmed that the selected test articles were not in vitro or clinically relevant inhibitors.

3.2 Determination of In Vitro Binding to Hepatocyte Medium and Metabolic Stability

A binding affinity equation was used to calculate the free fraction in media, $f_{u,in\ vitro}$ (Eq. 3). In the case of high PPB (> 96%), free concentrations were decreased (> 25%), which was accounted for by multiplying the nominal EC_{50} or $F2$ values by the calculated $f_{u,inc}$ (Table 1). Metabolic stability was determined during the last 24 hours of the incubation (Table 1). There was limited depletion (< 25% loss observed

when comparing the C_{avg} to the T_0 concentration) for acebilustat, delafloxacin, doravirine, lesinurad, raltegravir, rifampicin, rifaximin, tafamidis and tenofovir. A cut-off of > 25% was arbitrarily selected since it represents a change beyond typical bioanalytical assay variability. A correction factor of 0.2 was applied to nominal concentrations of pleconaril which undergoes nonspecific binding [15]. Pleconaril is also highly bound to plasma proteins (f_u 0.01) with an estimated $f_{u,in\ vitro}$ of 0.256. Several compounds in the dataset have reported PPB > 99%, including Cmpd 11 (f_u 0.003), Cmpd 2 (f_u 0.0007), efavirenz (f_u 0.0025), rilpivirine (f_u 0.003), selexipag (f_u < 0.01) and tafamidis (f_u 0.005). In these cases, the value for f_u was set to 0.01, as recommended in the regulatory guidance [10, 16, 17]. Other positive inducers which were 99% protein bound included Cmpd 7 and Cmpd 8. Correction of in vitro binding was made under the assumption that the in vitro medium was consistent with the study conditions employed here [contained 1.25 mg/ml bovine serum albumin (BSA)]. While this medium formulation is common, it is likely that some of the variability observed in the induction parameters derived between laboratories may be in part due to media formulation differences [18–20]. Of note, while this study did not investigate bosentan, rosiglitazone or pioglitazone, the calculated $f_{u,in\ vitro}$ predictions of 0.41, 0.25 and 0.16 compared well with observed $f_{u,in\ vitro}$ of 0.38, 0.22 and 0.15 for bosentan, pioglitazone and rosiglitazone, respectively [15].

3.3 Concentration Response Profiles

Increasing concentrations of many of the test compounds lead to increases in CYP3A4 mRNA in all donors evaluated (Fig. 1). Binimetinib, doravirine, lesinurad, rifaximin, rilpivirine, selexipag, tafamidis, tasimelteon and rifampicin resulted in concentration-dependent increases in all three donors. Some compounds resulted in “bell-shaped curves” as described in [8]. In that work, a recommendation was made to remove data points which showed a > 30% decrease in magnitude of induction when compared with the preceding concentration data due to suspected cytotoxicity. In the case of sofosbuvir, 300 μM data were removed from all donors to estimate the E_{\max} . For lesinurad, concentrations > 100 μM were excluded. In two cases there were different effects observed across donors, where rilpivirine showed signs of cytotoxicity > 30 μM in LLT and LDQ, but > 100 μM in donor YNZ. Delafloxacin was apparently cytotoxic in donor YNZ at concentrations > 100 μM , but not LDQ until 300 μM . Delafloxacin led to concentration-dependent increases in one of three donors (LLT); sofosbuvir led to concentration-dependent increases in two of three donors.

Table 1 Summary of derived in vitro binding parameters and metabolic stability results

Test article	$f_{u,p}$	$F_{u,inc}$	Mean depletion slope ($t_{1/2}$ h) across concentrations			Mean % loss across concentrations using measured C_{avg} compared to the nominal concentration		
			LLT	LDQ	YNZ	LLT	LDQ	YNZ
Acebilustat	NR	ND	-0.022 (31.2)	-0.013 (51.8)	-0.01 (67.8)	9.81	3.24	2.61
Binimetinib	0.03	0.51	-0.021 (33.0)	-0.030 (23.0)	-0.024 (28.9)	19.6	25.1	21.0
Delafloxacin	0.16	0.87	-0.0018 (380)	-0.0040 (174)	-0.0099 (70.4)	1.50	1.00	8.50
Doravirine	0.24	0.91	-0.0022 (320)	-0.014 (49.9)	-0.00056 (1236)	0.00	0.00	0.00
Lesinurad	0.02	0.41	-0.0089 (77.9)	-0.0025 (279)	-0.0023 (306)	4.05	1.23	1.82
Raltegravir	0.17	0.87	-0.024 (29.1)	-0.016 (42.8)	-0.026 (26.8)	21.4	15.8	22.6
Rifampicin	0.15	0.86	-0.010 (67.2)	-0.017 (40.3)	-0.021 (33.4)	10.6	16.8	19.5
Rifaximin	0.325	0.94	-0.0051 (136)	-0.0090 (76.6)	No loss observed	2.00	3.10	0.00
Rilpivirine	0.01	0.26	-0.048 (13.9)	-0.078 (8.84)	-0.069 (10.1)	33.8	41.0	39.5
Selexipag	0.01	0.26	-0.044 (15.7)	-0.022 (31.2)	-0.010 (68.7)	32.4	20.5	10.7
Sofosbuvir	0.39	0.96	-0.139 (4.99)	-0.032 (21.8)	-0.25 (27.7)	32.7	22.9	19.9
Tafamidis	0.01	0.26	-0.0028 (246)	No loss observed	-0.0041 (169)	0.00	0.00	0.00
Tasimeleone	0.10	0.79	-0.042 (16.6)	-0.025 (27.8)	-0.040 (17.5)	26.6	21.2	27.6
Tenofovir	0.99	1.00	-0.0046 (151)	-0.0034 (202)	-0.0036 (194)	3.40	0.00	3.30

$f_{u,p}$ fraction unbound plasma, $F_{u,inc}$ fraction unbound in incubation, *NR* not reported, *ND* not determined, C_{avg} concentration average, *LLT*, *LDQ* and *YNZ* donor designations assigned by the vendor from which they were purchased

3.4 Confirmation of True Negative In Vitro Inducers

True negative in vitro induction was confirmed by evaluating whether there was a statistically significant dose response and whether it translated to a meaningful fold induction over the tested concentrations. For the negative clinical inducers tested within this dataset, raltegravir, tenofovir and acebilustat were confirmed as true in vitro negatives in all three donors, whereas delafloxacin was negative in two donors and sofosbuvir negative in one donor (Table S6).

3.5 Induction Parameter Estimation

In the donors with concentration-dependent increases, the induction parameters could be estimated using the sigmoidal three-parameter model, Eq. (3), (Table 2). The average induction parameters were also calculated from the three donors and are designated as the “mean \pm SD.” The data presented in Table 2 represent the induction parameters estimated using the nominal (added) concentrations. Rifampicin was used as a positive control inducer, and the donor-derived induction parameters were used for the in vitro to in vivo extrapolation (*IVIVE*) assessment. The induction parameters were also corrected based on the average concentration over the incubation and considering the estimated in vitro binding (Table 1). In general, the donor designated LDQ resulted

in the highest magnitude of change (E_{max}) and the greatest potency (EC_{50}). Based on this, LDQ was the most sensitive donor. The other two donors showed similar E_{max}/EC_{50} values although there was variability in the absolute EC_{50} and E_{max} values derived across the three donors. Consistent with literature reports, the variability in interindividual donor response was as high as 20-fold for both EC_{50} and E_{max} values [4]. Of note, a similar magnitude of variability in intraindividual donor response was reported in the same paper. In contrast, repeat experiments (> 5) using these donors, within this laboratory, reproducibly yielded fold induction values of rifampicin at 10 μ M between 5 and 22% CV. By comparing the E_{max}/EC_{50} , the donor variability was reduced to within eightfold.

3.6 Compilation of Literature-Reported Data

To better understand where translation between true negative and true weak induction was most accurate, the induction parameters for “clean” inducers were collated [4]. Clean inducers were those which showed in vitro induction and were further determined to not be in vitro reversible or time-dependent inhibitors. This was to ensure that induction was treated in isolation of competing mechanisms of DDI. The parameters derived from the most sensitive donor are reported in Table 3.

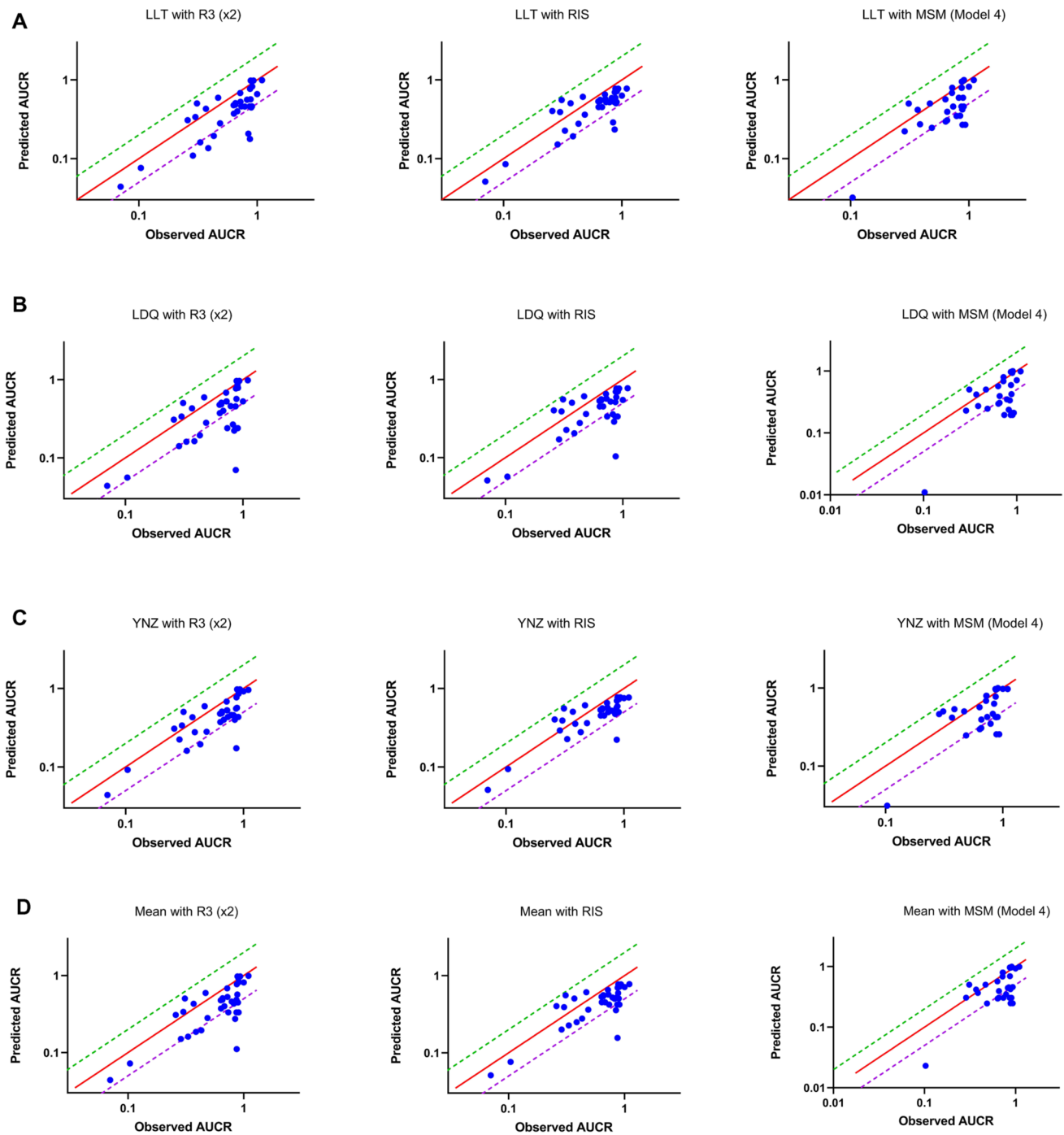


Fig. 2 Predicted versus observed change in AUC. The predicted AUC change (y -axis) was compared with the observed AUC change (x -axis) for the clinical induction set using the induction parameters derived for donor LLT, LDQ, YNZ and mean in combination with the induction parameters reported in Kenny et al. [4]. The red line represents the line of unity, and the dotted green line represents twofold above the observation; the purple dotted line represents twofold below the observation. The individual blue dots represent individual

clinical study results. The first panel shows the results when applying the R3 equation with $2 \times C_{\max,ss}$; the center panel shows the results when employing the generic RIS equation and the far right panel the results when applying the mechanistic static model using input parameters described as MSM 4. *AUCR* area under the curve ratio, $C_{\max,ss}$ unbound peak plasma concentration at steady state, R3 basic static model, RIS relative induction score, MSM mechanistic static model

Table 2 Summary of nominal derived induction parameters

Test article	Hepatocyte donor designation								
	LLT		LDQ		YNZ		Mean ± SD		
	EC_{50} (μM)	E_{max} fold	$F2$ (μM)	EC_{50} (μM)	E_{max} fold	$F2$ (μM)	EC_{50} (μM)	E_{max} fold	$F2$ (μM)
Bimimetinib	45.1	9.13	9.82	25.0	13.8	3.90	2.09	2.29	10.4
Delafloxacin	24.6	6.85	9.40	TN _{iv}	TN _{iv}	TN _{iv}	TN _{iv}	TN _{iv}	TN _{iv}
Doravirine	21.6	13	3.44	8.61	21.0	1.57	5.44	6.16	2.81
Lesinurad	5.70	18.8	0.659	2.57	9.63	1.2	8.40	10.1	1.55
Rifaximin	0.404	5.14	0.271	0.214	5.13	0.146	0.247	4.48	0.204
Rilpivirine	0.835	11.3	0.115	1.03	37.0	0.057	0.636	10.2	0.185
Selexipag	2.70	14.8	0.843	1.53	11.0	0.480	1.53	6.69	0.694
Sofosbuvir	TN _{iv}	TN _{iv}	TN _{iv}	4.98	7.90	2.53	2.00	2.61	5.63
Tafamidis	1.89	1.90	8.67	1.64	2.99	6.97	15.2	2.02	29.9
Tasimelteon	26.7	7.41	12.7	19.2	20.4	1.98	20.5	7.33	6.93
Rifampicin	0.663	14.8	0.0958	0.218	18.1	0.026	0.279	10.8	0.0595
Raltegravir	TN _{iv}	TN _{iv}	TN _{iv}	TN _{iv}	TN _{iv}	TN _{iv}	TN _{iv}	TN _{iv}	TN _{iv}
Tenofovir	TN _{iv}	TN _{iv}	TN _{iv}	TN _{iv}	TN _{iv}	TN _{iv}	TN _{iv}	TN _{iv}	TN _{iv}
Acebilustat	TN _{iv}	TN _{iv}	TN _{iv}	TN _{iv}	TN _{iv}	TN _{iv}	TN _{iv}	TN _{iv}	TN _{iv}

EC_{50} concentration eliciting half maximum fold induction, E_{max} maximal fold induction (fitted), $F2$ concentration producing twofold induction, TN_{iv} true negative in vitro, SD standard deviation, LLT , LDQ and YNZ donor designations assigned by the vendor from which they were purchased

3.7 Assessment of Correction Factor to F_2

The concentration resulting in twofold induction of mRNA (F_2) is proposed as a criteria in the EMA guideline on DDI [16]. Here, the in vitro induction is positive if a concentration-dependent increase greater than twofold ($> 100\%$)

Table 3 Summary of nominal in vitro parameters for true positive clinical inducers used in the analysis

Test article	Worst case hepatocyte donor data from Kenny et al. [4]		
	EC_{50} (μM)	E_{max} fold	F_2 (μM)
Bosentan	4.5	23.2	0.405
Clobazam	15.2	15.9	2.04
Lersivirine	20.7	11.5	3.94
Oxcarbazepine	105	6.12	41.0
Perampanel	10.6	25.5	0.864
Pleconaril	11.0	12.0	2.0
Rufinamide	288	10.4	61.3
Cmpd 1	1.06	27.5	4.73
Cmpd 2	4.02	17.65	0.483
Cmpd 3	58.6	25.79	4.73
Cmpd 7	1.05	4.589	0.583
Cmpd 8	13.4	4.224	8.33
Cmpd 11	1.77	30.51	0.120
Geometric mean values from Kenny et al. [4]			
Carbamazepine	31.3	12.7	5.35
Efavirenz	4.59	19.6	0.494
Phenytoin	30.0	10.8	6.12
Phenobarbital	261	16.7	33.2
Rifampicin	0.42	18.0	0.0565

EC_{50} concentration eliciting half maximum fold induction, E_{max} maximal fold induction (fitted), F_2 concentration producing twofold induction, *Cmpd* proprietary compound designation used as presented in [4]

Table 4 Summary of F_2 findings for the full in vitro inducer set (Tables 2 and 3) when corrected for metabolic stability and binding

Multiplier	LLT				LDQ				YNZ				Mean			
	FP	FN	PPE	NPE	FP	FN	PPE	NPE	FP	FN	PPE	NPE	FP	FN	PPE	NPE
50	11	0	0.28	0.00	12	0	0.30	0.00	11	0	0.28	0.00	12	0	0.30	0.00
30	10	0	0.26	0.00	12	0	0.30	0.00	10	0	0.26	0.00	10	0	0.26	0.00
20	9	0	0.24	0.00	10	0	0.26	0.00	9	0	0.24	0.00	10	0	0.26	0.00
15	9	0	0.24	0.00	9	0	0.24	0.00	9	0	0.24	0.00	10	0	0.26	0.00
12	8	0	0.22	0.00	8	0	0.22	0.00	7	0	0.20	0.00	9	0	0.24	0.00
10	8	0	0.22	0.00	8	0	0.22	0.00	7	0	0.20	0.00	9	0	0.24	0.00
5	6	2	0.19	0.13	6	2	0.19	0.13	6	2	0.19	0.13	7	2	0.21	0.13

The multiplier represents the number that the observed clinical $C_{\text{max,ss,u}}$ was multiplied by F_2 concentration producing twofold induction, *FP* false positives, *FN* false negative, *PPE* proportion of studies that were conducted unnecessarily, *NPE* proportion of studies that were not conducted but should have been, *LLT*, *LDQ* and *YNZ* donor designations assigned by the vendor from which they were purchased, $C_{\text{max,ss,u}}$ unbound peak plasma concentration at steady state

is observed at concentrations < 50 -fold the unbound C_{max} . Likewise, the data can be considered negative if $F_2/C_{\text{max,u}} < 50$. The ability to bin true positives and true negatives based on the F_2 value was evaluated at 50, 30, 20, 15, 12, 10 and $5 \times C_{\text{max,u}}$ (Table 4) as was the proportion of studies conducted unnecessarily (*PPE*) and the proportion of studies that were not conducted but should have been (*NPE*). For this assessment, the clinical studies were reduced to 28 TP and 16 TN by removing repeated dose levels of rifampicin (mean AUCR = 0.104 was used). When the induction parameter (F_2) was corrected for in vitro binding and metabolic stability, the maximum number of false positives could be reduced from 12 to 8 by decreasing the $C_{\text{max,u}}$ multiplier from 50 to 10 with no impact on the number of false negatives. When a correction factor of 5 was used, there were two false negatives including one of five trials with bosentan and oxcarbazepine. When the impact of binding or metabolic stability was not considered pleconaril was a false negative even at 50-fold $C_{\text{max,u}}$. When reported *PPB* values were used rather than f_u 0.01, efavirenz, *Cmpd* 11, *Cmpd* 2 and rilpivirine were all FN at cutoffs of 20, 5, 8 and sixfold $C_{\text{max,u}}$, respectively. There was some improvement in the number of FP when using the F_2 values derived from YNZ; however, this also corresponded to an increase in the number of FN values (Table S7). In general, the F_2 value reliably predicted true clinical induction using a cut-off value of 10.

3.8 Assessment of Correction Factor to R_3

The R_3 equation is proposed by the FDA and PMDA as an alternative basic model for evaluating the induction risk (Eq. 4), and at present it is recommended by both agencies to incorporate a tenfold correction factor to the $C_{\text{max,u}}$ [10, 16, 17]. Varying correction factors (10, 5, 2 and 0) were evaluated for application of the R_3 equation to determine

which value might reduce the number of FP while having no impact on the number of FN (Table 5). The clinical dataset contained 16 TN studies and 22 TP. When incorporating the individual induction parameters EC_{50} and E_{max} into the R3 equation with a correction factor of twofold to the $C_{max,u}$, there were no FNs. The best quantitative predictions were achieved with YNZ with 86.1% of the dataset falling within twofold of the predicted value and 33.3% falling between 0.8- and 1.25-fold of the observed. When there was no correction factor applied to the $C_{max,u}$, there was only one FN (pleconaril) across each donor, and the FP number could be reduced to 7. Having no correction factor also resulted in the best quantitative predictions measured by the GMFE closest to 1 and the lowest RMSE values. When the nominal induction parameters from the most quantitative donor were used there were two FNs, pleconaril and oxcarbazepine, and the number of FP was 5. In this case the accuracy of prediction improved from 86.1 to 91.7% within twofold and from 33.3 to 47.2% between 0.8 and 1.25-fold of the observed (Table 5 and Table S8). When reported PPB values were used rather than f_u 0.01, one trial of nine for efavirenz was considered a FN with twofold correction to $C_{max,u}$. Visual representations for the performance of the R3 equation are presented in Panels A of Fig. 2 for LLT, LDQ, YNZ and mean donor parameters, respectively.

3.9 Assessment of RIS and Proposed Cut-Off for AUCR

The relative induction score (RIS) is an alternative approach to evaluate induction risk which leverages the in vitro response derived from (Eq. 5) to the observed clinical data. The RIS curve established to support the data analysis in previous studies from the IQ IWG [4] (Eq. 6) was evaluated using the same clinical dataset used in the R3 analysis (16 TN and 22 TP). The best predictions were achieved when the parameters from donor YNZ were used. While there were still eight FPs, there were no FNs when a cut-off of < 0.7 for predicted AUCR was used (corresponding to 30% decrease in AUC). Additionally, up to 97% of predictions were within twofold of the observed (Table 6). Furthermore, using reported PPB values rather than 0.01 resulted in no FN. If the % decrease in AUC was shifted to 20% (AUCR = 0.8), then there were no FNs and the FP dropped from 9 to 8 for LDQ and from 8 to 5 for YNZ, using nominal derived induction parameters (Table S8). Visual representations for the performance of the R3 equation are presented in Panels B of Fig. 2 for LLT, LDQ, YNZ and mean donor parameters, respectively.

Table 5 Summary of R3 findings for the full in vitro inducer set (Tables 2 and 3) when corrected for metabolic stability and binding and using AUCR of < 0.8 as the positive cut-off value

Performance	LLT				LDQ				YNZ				Mean			
	×10	×5	×2	×0	×10	×5	×2	×0	×10	×5	×2	×0	×10	×5	×2	×
FP	10	10	9	8	11	11	10	8	11	9	8	7	12	11	9	8
FN	0	0	0	1	0	0	0	1	0	0	0	1	0	0	0	1
PPE	0.31	0.31	0.29	0.28	0.33	0.33	0.31	0.28	0.33	0.29	0.27	0.25	0.35	0.33	0.29	0.28
NPE	0.00	0.00	0.00	0.08	0.00	0.00	0.00	0.08	0.00	0.00	0.00	0.07	0.00	0.00	0.00	0.08
% 0.8–1.25×	11.1	19.4	27.8	50.0	8.33	16.7	27.8	41.7	13.5	25.0	33.3	52.8	8.11	18.9	29.7	43.2
%2×	27.8	41.7	83.3	91.7	25.0	38.9	72.2	83.3	32.4	44.4	86.1	94.4	32.4	43.2	78.4	91.9
%3×	50.0	86.1	94.4	97.2	52.8	80.6	88.9	97.2	59.5	88.9	97.2	97.2	54.1	83.8	97.3	97.3
# over	26	21	6	2	27	22	10	5	25	20	5	1	25	21	8	2
# under	0	0	0	1	0	0	0	1	0	0	0	1	0	0	0	1
GMFE	0.352	0.468	0.685	0.885	0.309	0.415	0.616	0.807	0.394	0.506	0.732	0.935	0.345	0.458	0.668	0.867
90% CI ±	0.48	0.46	0.42	0.40	0.55	0.52	0.48	0.45	0.46	0.43	0.40	0.39	0.49	0.46	0.43	0.41
RMSE	0.439	0.372	0.265	0.203	0.469	0.100	0.317	0.256	0.415	0.353	0.246	0.186	0.446	0.384	0.285	0.219

The multiplier (×10, ×5, ×2, ×0) represents the number that the observed clinical $C_{max,ss,u}$ was multiplied by R3 basic static model, AUCR area under the curve ratio, FP false positives, FN false negative, PPE proportion of studies that were conducted unnecessarily, NPE proportion of studies that were not conducted but should have been, %0.8–1.25× percent of studies where predicted AUCR over observed AUCR was between 0.8 and 1.25, %2× percent of studies where predicted AUCR over observed AUCR was within twofold, %3× percent of studies where predicted AUCR over observed AUCR was within threefold, # over number of clinical trials overpredicting induction > twofold, # under number of clinical trials underpredicting induction < twofold, GMFE geometric mean fold error, CI confidence interval, RMSE root mean square error, LLT, LDQ and YNZ donor designations assigned by the vendor from which they were purchased, AUCR area under the curve ratio, $C_{max,ss,u}$ unbound peak plasma concentration at steady state

Table 6 Summary of RIS findings for the full in vitro inducer set (Tables 2 and 3) when corrected for metabolic stability and binding and using AUCR of < 0.7 as the positive cut-off value

Performance	LDQ	LLT	YNZ	Mean
FP	9	9	8	9
FN	0	0	0	0
PPE	0.29	0.29	0.27	0.29
NPE	0.00	0.00	0.00	0.00
% 0.8–1.25×	19.4	22.2	30.6	18.9
%2×	83.3	91.7	97.2	89.2
%3×	97.2	97.2	97.2	97.3
# over	6	3	1	4
# under	0	0	0	0
GMFE	0.693	0.753	0.793	0.739
90% CI ±	0.44	0.39	0.38	0.40
RMSE	0.288	0.244	0.229	0.259

RIS relative induction score, AUCR area under the curve ratio, FP false positives, FN false negative, PPE proportion of studies that were conducted unnecessarily, NPE proportion of studies that were not conducted but should have been, %0.8–1.25× percent of studies where predicted AUCR over observed AUCR was between 0.8 and 1.25, %2× percent of studies where predicted AUCR over observed AUCR was within twofold, %3× percent of studies where predicted AUCR over observed AUCR was within threefold, # over number of clinical trials overpredicting induction > twofold, # under number of clinical trials underpredicting induction < twofold GMFE geometric mean fold error, CI confidence interval, RMSE root mean square error, LLT, LDQ and YNZ donor designations assigned by the vendor from which they were purchased

3.10 Assessment of the Mechanistic Static Model (MSM)

Regulatory agencies include the MSM as a basic method for clinical induction risk but recommend that it not be used for combined mixed mechanism (i.e., inhibition and induction) predictions. Since the in vitro inducers selected in this study were not mixed mechanism perpetrators, only the induction portion of the MSM was included. The entire clinical dataset was used for the MSM since it considers substrate specificity in the equation and includes 16 TN trials and 64 TPs. For direct comparison of MSM4 with the R3 and RIS models, the dataset was also reduced to align the clinical trials tested. The proprietary compounds collected by the IQ-IWG did not include data needed to calculate the hepatic inlet concentration (dose or MW), so they were excluded from the analysis, resulting in 16 TN and 16 TP studies. The MSM strongly overpredicted the clinical induction risk particularly as written in the DDI guidelines (Model 1), with all donors resulting in a high FP rate (15 or 16/16 TN trials) and minimal quantitative accuracy. There were two underpredictions when using budesonide as the CYP3A substrate and rifampicin

as the strong inducer. Budesonide is strongly induced by rifampicin, to a greater extent than midazolam (decrease in AUC of 99.7% vs. ~ 90%, respectively). The MSM accurately predicts a strong induction but underpredicts the magnitude when comparing AUCR. Modifying the gut concentrations based on PPB (Model 2) slightly improved the predictions but they were still largely overpredicted. Further modification of input parameters, including using the unbound maximum hepatic inlet concentration as the gut concentration and unbound systemic concentration as the hepatic input (Model 3), resulted in reduction of FP and iterative improvement in the quantitative risk assessment; however, there was still a tendency for strong overprediction of induction magnitude. Applying the average concentrations rather than the maximal concentrations (Model 4), which is more aligned with PBPK dynamic modeling approaches, provided the best quantitative prediction of all the MSM evaluated and resulted in 0 FNs (Table 7). Model 4 was applied to the same dataset used in the R3 and RIS analysis to enable direct comparisons of performance (Table 8). Model 4 resulted in a comparable number of FPs but slightly lower GMFE and %within quantitative accuracies and higher numbers of overpredictions than both the RIS and R3 models. When considering the desire to limit the number of FNs, decrease the number of FPs and improve the quantitative accuracy, the basic model ranking followed RIS > R3 ($2 \times C_{\max,ss}$) > MSM (Model 4). Visual representations for the performance of the R3 equation are presented in Panels C of Fig. 2 for LLT, LDQ, YNZ and mean donor parameters, respectively. The full dataset which incorporated similar dose levels with different substrates used for the positive inducers is displayed in Fig. 3.

3.11 Internal Calibration of Induction Parameters Considering the Simcyp Approach and Provided Parameters for Rifampicin

An additional method, proposed for PBPK modeling, includes calibration of the in vitro derived induction parameters with those reported for rifampicin, the goal being to reduce the contribution of inter-donor variability on the magnitude of induction achieved. In this approach, the optimized EC_{50} and E_{\max} values used for rifampicin within Simcyp ($EC_{50} = 0.32$ and $E_{\max} = 16$) are divided by the observed values to determine donor-specific scalars of each parameter, which are then applied to those parameters derived from the other inducers. For this evaluation, the mean data were used (Tables S9 and S10). There was a tendency for the calibrated data to provide a more conservative measure of induction risk, resulting in a greater number of FP values, increased overestimations, decreased quantitative accuracy and GMFE and increased RMSE.

Table 7 Summary of MSM findings using the full dataset and various input parameters

Performance	LLT				LDQ				YNZ				Mean			
	M1	M2	M3	M4	M1	M2	M3	M4	M1	M2	M3	M4	M1	M2	M3	M4
FP	15	12	11	10	15	13	11	10	15	11	10	9	16	13	11	9
FN	0	0	0	0	0	0	0	0	0	0	0	0	0	0	0	0
PPE	0.21	0.17	0.16	0.15	0.21	0.18	0.16	0.15	0.21	0.16	0.15	0.13	0.22	0.18	0.16	0.13
NPE	0.00	0.00	0.00	0.00	0.00	0.00	0.00	0.00	0.00	0.00	0.00	0.00	0.00	0.00	0.00	0.00
% 0.8–1.25×	0.00	5.48	12.3	27.4	0.00	5.41	10.8	17.8	2.74	8.22	12.3	30.1	0	6.76	13.5	21.9
%2×	6.85	16.4	26.0	54.8	0.00	13.5	20.3	30.1	11.0	21.9	34.2	60.2	4.05	14.9	23.0	50.7
%3×	20.5	30.1	53.4	79.4	12.3	24.3	32.4	53.4	28.8	41.1	64.4	75.3	21.6	31.1	45.9	68.5
# over	66	59	52	31	71	62	57	49	63	55	46	27	69	61	55	34
# under	2	2	2	2	2	2	2	2	2	2	2	2	2	2	2	2
GMFE	0.142	0.192	0.319	0.592	0.106	0.143	0.225	0.347	0.199	0.264	0.406	0.619	0.140	0.188	0.305	0.509
90% CI ±	0.682	0.692	0.641	0.536	0.688	0.737	0.710	0.648	0.641	0.647	0.592	0.532	0.651	0.673	0.632	0.562
RMSE	0.460	0.411	0.322	1.27	0.477	0.427	0.353	1.36	0.443	0.391	0.290	1.16	0.468	0.419	0.329	1.27

MSM mechanistic static model, *FP* false positive, *FN* false negative, *PPE* proportion of studies that were conducted unnecessarily, *NPE* proportion of studies that were not conducted but should have been, %0.8–1.25× percent of studies where predicted AUCR over observed AUCR was between 0.8 and 1.25, %2× percent of studies where predicted AUCR over observed AUCR was within twofold, %3× percent of studies where predicted AUCR over observed AUCR was within threefold, # *over* number of clinical trials overpredicting induction > twofold, # *under* number of clinical trials underpredicting induction < twofold, *GMFE* geometric mean fold error, *CI* confidence interval, *RMSE* root mean square error, *LLT*, *LDQ* and *YNZ* donor designations assigned by the vendor from which they were purchased, *M1* using gut concentration and unbound hepatic inlet as input parameters as described in regulatory guidance, *M2* inputting gut concentration corrected with $f_{u,p}$ and unbound hepatic inlet, *M3* inputting unbound hepatic inlet as the gut concentration and unbound $C_{max,ss}$ as the hepatic concentration, *M4* inputting the unbound average hepatic inlet concentration as the gut concentration and the average unbound concentration as the hepatic concentration, *AUCR* area under the curve ratio, $C_{max,ss,u}$ unbound peak plasma concentration at steady state

Table 8 Summary of MSM Model 4 findings using the same dataset as R3 and RIS

Performance	LLT	LDQ	YNZ	Mean
FP	9	9	8	9
FN	0	0	0	0
PPE	0.36	0.36	0.33	0.36
NPE	0.00	0.00	0.00	0.00
% 0.8–1.25×	40.0	40.0	43.3	45.2
%2×	73.3	60.0	70.0	64.5
%3×	96.7	73.3	90.0	87.1
# over	8	12	9	11
# under	0	0	0	0
GMFE	0.686	0.581	0.734	0.664
90% CI ±	0.467	0.577	0.493	0.496
RMSE	1.28	1.41	1.23	1.37

MSM mechanistic static model, *R3* basic static model, *RIS* relative induction score, *FP* false positive, *FN* false negative, *PPE* proportion of studies that were conducted unnecessarily, *NPE* proportion of studies that were not conducted but should have been, %0.8–1.25× percent of studies where predicted AUCR over observed AUCR was between 0.8 and 1.25, %2× percent of studies where predicted AUCR over observed AUCR was within twofold, %3× percent of studies where predicted AUCR over observed AUCR was within threefold, # *over* number of clinical trials overpredicting induction > twofold, # *under* number of clinical trials underpredicting induction < twofold, *GMFE* geometric mean fold error, *CI* confidence interval, *RMSE* root mean square error, *LLT*, *LDQ* and *YNZ* donor designations assigned by the vendor from which they were purchased

3.12 Evaluation of Performance for Expanded Positive Inducer Set

Use of rifampicin is currently restricted because of the presence of a potentially carcinogenic impurity 1-methyl-4-nitrosopiperazine (MNP), with recommended intake levels below those detected in available batches precluding its use as a strong inducer [21]. Other strong inducers including carbamazepine and phenytoin have been proposed as potential alternatives, as has the possibility to use moderate inducers to better understand the impact of induction on a CYP3A substrate. To evaluate the translation of the proposed models to these positive clinical inducers, the geometric mean values from the IQ-IWG [4] paper were used in the assessment as they resulted in the best predictions for quantitative risk assessment (compared with worst case donor, mean and median values) (Table 3). In total, 22 additional clinical studies were collected, with 5 TP for carbamazepine (AUCR range 0.124–0.603), 9 TP and 3 TN for efavirenz (AUCR range 0.240–0.929), 1 TP study with phenobarbital (AUCR = 0.394 with nifedipine) and 4 TP studies for phenytoin (AUCR range 0.105–0.607). All TP studies were appropriately binned using an *F2* cut-off value of $10 \times C_{max,u}$. When applying the *R3* equation with a twofold correction factor, three of the five carbamazepine studies were predicted within

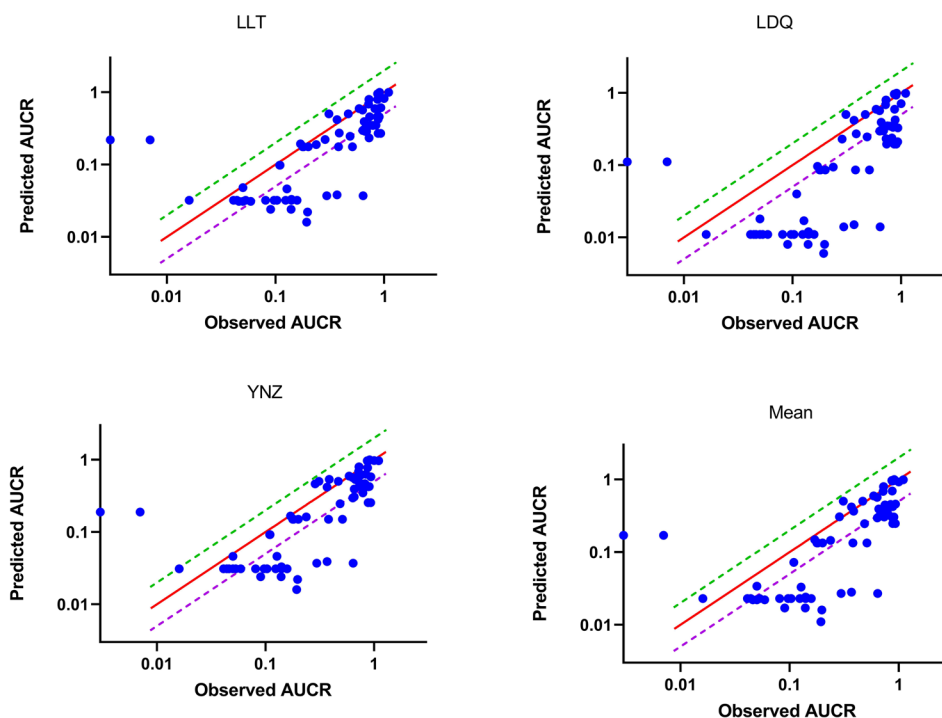


Fig. 3 Predicted versus observed change in AUC for an expanded substrate set using mechanistic static model 4. The predicted AUC change (y-axis) was compared with the observed AUC change (x-axis) for the clinical induction set using the induction parameters derived for the average donor induction parameters in combination with the induction parameters reported in Kenny et al. [4]. The red line represents the line of unity, and the dotted green line represents

twofold above the observation; the purple dotted line represents twofold below the observation. The individual blue dots represent individual clinical study results. The upper left panel shows the results for donor LLT, the upper right shows the results for donor LDQ, the lower left shows the results for donor YNZ, and the lower right shows the results when applying the average donor induction parameters. AUCR area under the curve ratio

twofold of the observed. All the efavirenz studies except one were predicted within twofold although the three TN studies were FP. The phenobarbital study was correctly predicted. Three of the four phenytoin studies were predicted within twofold. The RIS model yielded very similar observations as the R3 equation with 81.8% of studies predicted within twofold. The MSM 4 was the only model able to accurately capture two of the three TN efavirenz studies and quantitatively predicted the results with 77.3% within twofold. Overall, the recommendations made from the results of the clean inducer set were consistent with the outcome of the expanded true positive inducer set. In addition, the data demonstrate that for carbamazepine and efavirenz, which both show reversible inhibition of CYP3A *in vitro*, using the induction parameters alone, predict the observed clinical outcome well. Calibration to rifampicin was also investigated and consistent with the observations from the clean inducers tended to provide a more conservative estimate of risk (Table S11). Visual representations for the performance of the equations are presented in Figs. S2 and S3 for the mean donor parameters, with and without rifampicin calibration, respectively.

4 Discussion and Conclusion

The potential for drug-drug interactions (DDI) is often evaluated as part of early discovery and development using a series of well-defined *in vitro* assays. The relative importance of any DDI liability is considered among a plethora of additional factors; therefore, it is not uncommon to accept a potential DDI as part of a comprehensive data package aligned to effectively address patient needs. Therefore, to aid informed decision making, including the appropriate timing of clinical DDI studies, it is of great interest to identify accurate translation of *in vitro* DDI data for projection of clinical outcome.

There have been numerous publications evaluating the translation of *in vitro* derived induction parameters to predict clinical risk [1, 2, 4, 22, 23]. Of note, despite a tendency for overprediction, there were still several false negative inducers when applying the basic models without consideration of *in vitro* binding or stability [4]. False negatives included dexamethasone, pleconaril, oxcarbazepine, Cmpd 2, 11, 15, efavirenz, lopinavir, nevirapine and troglitazone.

Dexamethasone is a unique outlier in that hepatocyte incubations for in vitro induction studies typically contain low levels, which are added to promote phenotypic architecture, suppress proliferation, inhibit induction of stress signaling pathways and aid in expression of liver-enriched transcription factors, including those nuclear receptors required for DMET induction [24–29]. Thus, it is likely that the dexamethasone parameters are under (E_{\max}) or over (EC_{50}) estimated under standard incubation conditions.

In line with the regulatory recommendations, a maximal value of 0.01 was applied for f_u . When reported binding values were used, there was an increase in FN values using the $F2$ equation with $10\times C_{\max,u}$ including all trials with efavirenz. There were no FNs using the RIS approach. Metabolic stability, as recommended in the EMA guideline [16], was also included. While there is no guidance offered on how to apply these data, there is emerging literature evidence that it is important to consider the temporal nature of both induction time course and concentration of the inducer [8, 15, 30]. The data generated within this paper suggest that to reduce the potential for false negatives both the in vitro binding and the metabolic stability should be considered in derivation of the induction parameters. The use of C_{av} with the proposed cut-off of > 25% loss and > 25% reduction in unbound free fraction appears reasonable.

When comparing the predicted AUCR, the MSM yielded underpredictions for rifampicin with budesonide as the substrate. Rifampicin strongly decreases the AUCR of budesonide with reported AUCR of 0.003 and 0.007. The most sensitive donor projection was 0.111, which when compared directly with the observed AUCR corresponds to a 37-fold underprediction. Of note, all the rifampicin predictions are within 0.8 to 1.25-fold of observations when the %decrease in AUC is compared rather than the AUCR. It would be valuable to better understand this lack of concordance and what endpoint (i.e., AUCR vs. %decrease in AUC) is more meaningful to compare.

There are limitations of the analysis conducted herein including that assumptions were made to the correction of the positive control values based on literature data and that the dataset was limited to induction only interactions. Despite these limitations, the analysis demonstrates that reducing the correction factors to basic equations can result in improved accuracy of predictions and point to $10\times$ and $2\times$ for $F2$ and $R3$ equations, respectively. In addition, the best quantitative accuracy was achieved when using the RIS model with an AUCR cut-off of < 0.7 as positive. Lastly, the accuracy of the MSM was improved when the average inlet concentration was used for the gut portion and the average unbound systemic concentration was used for the hepatic input concentration, which is consistent with a recent report evaluating prediction methods for TDI of CYP3A [13].

Supplementary Information The online version contains supplementary material available at <https://doi.org/10.1007/s13318-022-00763-y>.

Acknowledgements The authors acknowledge Drs. Natalie Hosea, Amin Kamel and Suresh K. Balani for critical review of the manuscript and data interpretation, Darian Bartkowski for generating the metabolic stability data and the ICH M12 working group members including Drs. Niresh Hariparsad, Heidi Einolf, Theunis Goosen, Xinning Yang and Carolien Versantvoort for helpful discussions.

Declarations

Funding This study was sponsored by Takeda Development Center Americas, Ltd.

Conflict of interest DR and CLF are/were employees of Takeda Development Center Americas, Inc., and receive stock or stock options.

Ethical approval Not applicable.

Availability of data and materials All data and analysis generated during these studies are included in this article (and its supplementary information) or are available upon request to the corresponding author.

Code availability Not applicable.

Consent to participate Not applicable.

Consent to publish Not applicable.

Author contributions Participated in research design: DR and CLF. Conducted experiments: CLF. Performed data analysis: DR. Wrote or contributed to the writing of the manuscript: DR and CLF.

Open Access This article is licensed under a Creative Commons Attribution-NonCommercial 4.0 International License, which permits any non-commercial use, sharing, adaptation, distribution and reproduction in any medium or format, as long as you give appropriate credit to the original author(s) and the source, provide a link to the Creative Commons licence, and indicate if changes were made. The images or other third party material in this article are included in the article's Creative Commons licence, unless indicated otherwise in a credit line to the material. If material is not included in the article's Creative Commons licence and your intended use is not permitted by statutory regulation or exceeds the permitted use, you will need to obtain permission directly from the copyright holder. To view a copy of this licence, visit <http://creativecommons.org/licenses/by-nc/4.0/>.

References

1. Einolf HJ, et al. Evaluation of various static and dynamic modeling methods to predict clinical CYP3A induction using in vitro CYP3A4 mRNA induction data. *Clin Pharmacol Ther.* 2014;95(2):179–88.
2. Shou M, et al. Modeling, prediction, and in vitro in vivo correlation of CYP3A4 induction. *Drug Metab Dispos.* 2008;36(11):2355–70.
3. Almond LM, et al. Prediction of drug–drug interactions arising from CYP3A induction using a physiologically based dynamic model. *Drug Metab Dispos.* 2016;44(6):821–32.

4. Kenny JR, et al. Considerations from the innovation and quality induction working group in response to drug–drug interaction guidances from regulatory agencies: focus on CYP3A4 mRNA in vitro response thresholds, variability, and clinical relevance. *Drug Metab Dispos.* 2018;46(9):1285–303.
5. Fahmi OA, et al. Evaluation of CYP2B6 induction and prediction of clinical drug–drug interactions: considerations from the IQ consortium induction working group—an industry perspective. *Drug Metab Dispos.* 2016;44(10):1720–30.
6. Lutz JD, et al. Cytochrome P450 3A induction predicts P-glycoprotein induction; part 2: prediction of decreased substrate exposure after rifabutin or carbamazepine. *Clin Pharmacol Ther.* 2018;104(6):1191–8.
7. Sane RS, et al. Contribution of Major metabolites toward complex drug–drug interactions of deleobuvir: in vitro predictions and in vivo outcomes. *Drug Metab Dispos.* 2016;44(3):466–75.
8. Wong SG, et al. Considerations from the innovation and quality induction working group in response to drug–drug interaction guidance from regulatory agencies: guidelines on model fitting and recommendations on time course for in vitro cytochrome P450 induction studies including impact on drug interaction risk assessment. *Drug Metab Dispos.* 2021;49(1):94–110.
9. Yates P, et al. Statistical methods for analysis of time-dependent inhibition of cytochrome p450 enzymes. *Drug Metab Dispos.* 2012;40(12):2289–96.
10. FDA (2020) In vitro drug interaction studies—cytochrome P450 enzyme- and transporter-mediated drug interaction guidance for industry
11. Fahmi OA, et al. A combined model for predicting CYP3A4 clinical net drug–drug interaction based on CYP3A4 inhibition, inactivation, and induction determined in vitro. *Drug Metab Dispos.* 2008;36(8):1698–708.
12. Isoherranen N, et al. Importance of multi-p450 inhibition in drug–drug interactions: evaluation of incidence, inhibition magnitude, and prediction from in vitro data. *Chem Res Toxicol.* 2012;25(11):2285–300.
13. Tseng E, et al. Static and dynamic projections of drug–drug interactions caused by cytochrome P450 3A time-dependent inhibitors measured in human liver microsomes and hepatocytes. *Drug Metab Dispos.* 2021;49:947–60.
14. Vieira ML, et al. Evaluation of various static in vitro-in vivo extrapolation models for risk assessment of the CYP3A inhibition potential of an investigational drug. *Clin Pharmacol Ther.* 2014;95(2):189–98.
15. Sun Y, et al. Quantitative prediction of CYP3A4 induction: impact of measured, free, and intracellular perpetrator concentrations from human hepatocyte induction studies on drug–drug interaction predictions. *Drug Metab Dispos.* 2017;45(6):692–705.
16. EMA (2012) Guideline on the investigation of drug interactions
17. PMDA (2018) Pharmaceuticals and Medical Devices Agency (Japan): drug interaction guideline for drug development and labelling recommendations
18. Madan A, et al. Effects of prototypical microsomal enzyme inducers on cytochrome P450 expression in cultured human hepatocytes. *Drug Metab Dispos.* 2003;31(4):421–31.
19. Nishimura M, et al. Comparison of inducibility of CYP1A and CYP3A mRNAs by prototypical inducers in primary cultures of human, cynomolgus monkey, and rat hepatocytes. *Drug Metab Pharmacokinet.* 2007;22(3):178–86.
20. Runge D, et al. Induction of cytochrome P450 (CYP)1A1, CYP1A2, and CYP3A4 but not of CYP2C9, CYP2C19, multidrug resistance (MDR-1) and multidrug resistance associated protein (MRP-1) by prototypical inducers in human hepatocytes. *Biochem Biophys Res Commun.* 2000;273(1):333–41.
21. FDA 2020. <https://www.fda.gov/drugs/drug-safety-and-availability/fda-updates-and-press-announcements-nitrosamines-rifampin-and-rifapentine>. Accessed 15 Nov 2021.
22. Tsutsui H, Kuramoto S, Ozeki K. Evaluation of methods to assess CYP3A induction risk in clinical practice using in vitro induction parameters. *Biol Pharm Bull.* 2021;44(3):338–49.
23. Zhang JG, et al. Evaluation of calibration curve-based approaches to predict clinical inducers and noninducers of CYP3A4 with plated human hepatocytes. *Drug Metab Dispos.* 2014;42(9):1379–91.
24. Dasgupta A, et al. E-cadherin synergistically induces hepatocyte-specific phenotype and maturation of embryonic stem cells in conjunction with hepatotrophic factors. *Biotechnol Bioeng.* 2005;92(3):257–66.
25. Ezzell RM, et al. Effect of collagen gel configuration on the cytoskeleton in cultured rat hepatocytes. *Exp Cell Res.* 1993;208(2):442–52.
26. Li WC, et al. Keratinocyte serum-free medium maintains long-term liver gene expression and function in cultured rat hepatocytes by preventing the loss of liver-enriched transcription factors. *Int J Biochem Cell Biol.* 2007;39(3):541–54.
27. Olsavsky Goyak KM, Laurenzana EM, Omiecinski CJ. Hepatocyte differentiation. *Methods Mol Biol.* 2010;640:115–38.
28. Pascussi JM, et al. Dexamethasone enhances constitutive androstane receptor expression in human hepatocytes: consequences on cytochrome P450 gene regulation. *Mol Pharmacol.* 2000;58(6):1441–50.
29. Sidhu JS, Liu F, Omiecinski CJ. Phenobarbital responsiveness as a uniquely sensitive indicator of hepatocyte differentiation status: requirement of dexamethasone and extracellular matrix in establishing the functional integrity of cultured primary rat hepatocytes. *Exp Cell Res.* 2004;292(2):252–64.
30. Chang C, et al. An exposure-response analysis based on rifampin suggests CYP3A4 induction is driven by AUC: an in vitro investigation. *Xenobiotica.* 2017;47(8):673–81.